J Solid State Electrochem (2009) 13:485–496
DOI 10.1007/s10008-008-0583-6

ORIGINAL PAPER

Electrocatalytic reduction of NAD^+ at glassy carbon electrode modified with single-walled carbon nanotubes and Ru(III) complexes

Abdollah Salimi · Mohadeseh Izadi · Rahman Hallaj · Saied Soltanian · Hassan Hadadzadeh

Received: 27 January 2008 / Accepted: 6 May 2008 / Published online: 10 June 2008
© Springer-Verlag 2008

Abstract A simple procedure was developed to prepare a glassy carbon electrode modified with carbon nanotubes and Ruthenium (III) complexes. First, 25 μl of dimethyl sulfoxide–carbon nanotubes solutions (0.4 mg/ml) was cast on the surface of the glassy carbon electrode and dried in air to form a carbon nanotube film at the electrode surface. Then, the glassy carbon/carbon nanotube-modified electrode was immersed into a Ruthenium (III) complex solution (direct deposition) for a short period of time (10–20 s for multiwalled carbon nanotubes and 20–40 s for single-walled carbon nanotubes). The cyclic voltammograms of the modified electrode in aqueous solution shows a pair of well-defined, stable, and nearly reversible redox couple, Ru (III)/Ru(II), with surface-confined characteristics. The attractive mechanical and electrical characteristics of carbon nanostructures and unique properties and reactivity of Ru complexes are combined. The transfer coefficient (α), heterogeneous electron transfer rate constants (k_s), and surface concentrations (Γ) for the glassy carbon/single-walled carbon nanotubes/Ru(III) complex-, glassy carbon/multiwalled carbon nanotubes/Ru(III) complex-, and glassy carbon/Ru(III) complex-modified electrodes were calculated using the cyclic voltammetry technique. The modified electrodes showed excellent catalytic activity, fast response time, and high sensitivity toward the reduction of nicotinamide adenine dinucleotide in phosphate buffer solutions at a pH range of 4–8. The catalytic cathodic current depends on the nicotinamide adenine dinucleotide concentration. In the presence of alcohol dehydrogenase, the modified electrode exhibited a response to addition of acetaldehyde. Therefore, the main product of nicotinamide adenine dinucleotide electroreduction at the Ru(III) complex/carbon nanotube-modified electrode was the enzymatically active NADH. The purposed sensor can be used for acetaldehyde determination.

Keywords CNTs · Ru(III) complexes · Glassy carbon · NAD^+ · Alcohol dehydrogenase · Acetaldehyde · Sensor

A. Salimi (✉) · M. Izadi · R. Hallaj
Department of Chemistry, University of Kurdistan,
P.O. Box 416, Sanandaj, Iran
e-mail: absalimi@yahoo.com

A. Salimi · S. Soltanian
Research Center for Nanotechnology,
University of Kurdistan,
P.O. Box 416, Sanandaj, Iran

H. Hadadzadeh
Department of Chemistry, Isfahan University of Technology,
Isfahan, Iran

Introduction

Nicotinamide adenine dinucleotide (NAD^+) is a ubiquitous cofactor, used by more than 300 dehydrogenase enzymes. The electrochemical reduction of NAD^+ to the enzymatically active form nicotinamide adenine dinucleotide (NADH) has attracted considerable attention due to the industrial and biomedical importance of reduced derivatives of adenine. Furthermore, electrochemical reduction of NAD^+ is known to be an efficient means for this purpose and has potential application for fabrication of biosensors. In addition, the high cost of NADH to a bioreactor has been the major motivation for research in the development of in situ NADH regeneration techniques. The NAD^+/NADH redox couple has a formal potential of −0.32 V vs. the standard hydrogen electrode (pH7), but its direct reduction requires a large overpotential [1]. The direct reduction of

NAD^+ on unmodified metallic electrodes results mostly in the formation of an inactive dimmer NAD_2, which can be only partially protonated and further reduced to both 1,4- and 1,6-NADH at significantly higher negative overpotentials [2, 3]. Among these products, only the 1,4-NADH is active in enzyme-coupled reactions, and the indirect electrocatalytic reduction of the NAD^+ seems to be a better way to decrease the overpotential and to get a high yield of 1,4-NADH [4]. The fast dimerization reaction, coupled with the slow second reaction step, is the major reason for the direct reduction of NAD^+ on unmodified electrodes, which results in the formation of NAD_2 rather than enzymatically active NADH ([5] and references there in). Numerous modified electrodes based on the use of different electron transfer mediators such as cerium hexachloroplatinate [6], iron hexachloroplatinate [7], flavine adenine dinucleotide (FAD)-modified zinc oxide film [8], poly-natural red [9, 10], poly(3-methylthiophene)/phenol [11], poly-pyrrole rhodium bis-terpyridine [12], ruthenium-modified glassy carbon (GC) electrode[13], and poly-crystalline gold electrode [14] have been used for the electrocatalytic reduction of NAD^+. Furthermore, electrochemical properties of NAD^+/NADH redox couple on hybrid poly-(luminal)/FAD film [15] and nordihydroguaiaretic acid/FAD hybrid film [16] have been investigated. In addition, the reduction of NAD^+ to NADH on electrodes modified by a layer of immobilized methyl viologen and lipoamide dehydrogenase [17, 18], methyl viologen, and diphorase [19, 20] have been reported. Although enzymatic modification of an electrode surface gives encouraging results in the reduction of NAD^+ to enzymatically active 1,4-NADH, this approach results in a rather complex electrode system due to difficulties related to the immobilization of an enzyme mediator at the electrode surface, lack of stability, and loss of the enzyme activity due to the intrinsic nature of the enzyme, electron mediator leakage, and slow NADH regeneration rate. Moreover, high cost and low reproducibility and repeatability are other disadvantages of enzyme electrodes. Hence, it is pertinent to develop a simple and reliable method for the modification of the electrode surface using new electron transfer mediators, which would allow electrochemical regeneration of an enzymatically active form of NADH.

Ruthenium is a remarkable transition metal that displays different oxidation states, which make wide variations of redox reactions possible [21–24]. Owing to its reversible redox activity and excellent electrocatalytic properties, Ru complexes have received considerable attention in the field of electroanalysis and fabrication of chemically modified electrodes [13, 25–32]. The modification of different electrode surfaces with Ru complexes is possible in several ways such as adsorption and entrapping into the carbon paste, conductive composites, and polymer matrix.

Carbon nanotubes (CNTs) are a new kind of nanostructure material, which is promising as an immobilization substance because of its significant mechanical strength, high surface area, excellent electrical conductivity, and good chemical stability [33]. Recently, many efforts have been focused on the fictionalizations of CNTs with various molecules by using covalent or noncovalent approaches to obtain desired properties [34–38]. Among these approaches, the fictionalization of the side walls of CNTs in the noncovalent way is an effective way to preserve the sp^2 nanotube structure and thus their electronic characteristics. In addition, the strong interaction of aromatic groups with π-staking of CNTs is a similar manner to achieve the desired purpose. Immobilization of molecules and biomolcules on CNTs has been pursued in the past, motivated by the prospects of using nanotubes as new types of sensor and biosensors. Due to electronic and specific recognition properties of CNTs as immobilized systems, they can be used for making ideal miniaturized sensors. The surface of CNTs can be chemically modified to impart a specific desired property, either covalently or physically adsorption [39–42]. The compatibility and electrochemical applications of CNTs to immobilize a variety of species on the external and internal surfaces of them have been reported [41–47]. It was shown earlier that the electrocatalytic properties of CNTs toward other slow redox systems can be improved by coupling metal centers with them [48, 49].

Recently, we used CNT-modified electrodes for the immobilization of different electron transfer mediators and their application in sensors and biosensors fabrication [50–54]. In the current study, a simple and fast procedure was used for immobilization of Ru(III) complexes on a GC electrode modified with CNTs and their application for electrocatalytic reduction of NAD^+. The electron transfer rate constants of the Ru(III)/Ru(II) redox couple and the catalytic rate constant of the modified electrode for NAD^+ reduction were also evaluated and calculated. The ability of the modified electrode for the fabrication of an acetaldehyde biosensor was evaluated.

Experimental

Chemical and reagents The Ru(III) complexes used in this study (Scheme 1) were $[Ru(trpy)Cl_3]$ (where trpy = 2,2′-6′,2″-terpyridine), $[Ru(NH_3)_5(2,4,5\text{-}Cl_3pcyd)](ClO_4)_2$ (where 2,4,5-Cl_3pcyd = 2,4,5-trichloro phenylcyanamide anion), and $[Ru(phen)_2(phen\text{-}dioxime)](PF_6)_2$ (where phen = 1,10-phenanthroline and Phen-dioxime = 1,10-phenanthroline-5,6-dioxime), which were synthesized, purified, and characterized as reported [55–57]. NAD^+ with purity of 95% was from Sigma and used without further purification. Alcohol dehydrogenase (ADH; EC 1.1.1.1., from Baker's Yeast) was purchased from Sigma. Acetonitrile

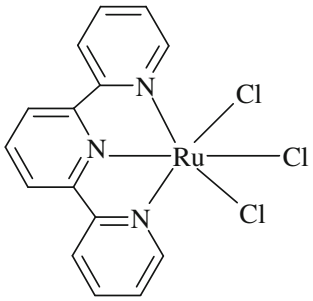

Complex (A)

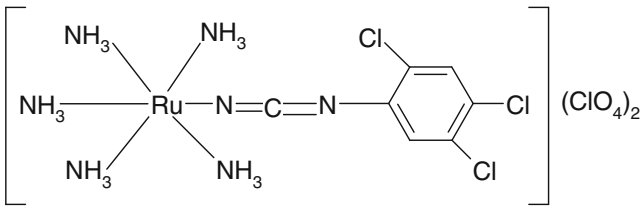

Complex (B)

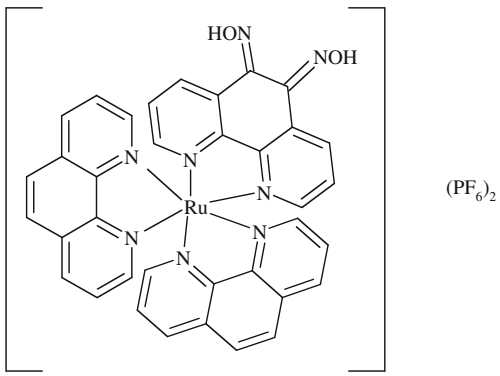

Complex (C)

Scheme 1. The structures of used complexes

(ACN) and dimethyl sulfoxide (DMSO) were from Merck. Multiwall CNTs (MWCNTs) with 95% purity (10–20 nm diameter) and 1 μm length were obtained from Nanolab (Brighton, MA, USA). Single-wall CNTs (SWCNTs) have been manufactured by CNI (USA). Double-distillate water was used to prepare all solutions. Buffer solutions (0.1 M) were prepared from H_2SO_4, H_3PO_4, NaH_2PO_4, and Na_2HPO_4. Hydrogen chloride (HCl) and sodium hydroxide (NaOH) were used for pH adjustment. Solutions were deaerated by bubbling high purity (99.99%) of argon gas through them prior to the experiments. All electrochemical experiments were carried out at room temperature 25 ± 0.1 °C.

Apparatus and procedures Electrochemical experiments were performed with a computer controlled μ-Autolab modular electrochemical system (Eco Chemie, Ultecht, The Netherlands), driven with a general-purpose electrochemical system software (Eco Chemie). A conventional three-electrode cell was used with a Ag/AgCl/(saturated KCl) as the reference electrode, a Pt wire as a counterelectrode, and a GC disk (modified and unmodified) as a working electrode. Voltammetry on electrodes coated with Ru complex–CNTs was done in buffers containing no complex. All of the used electrodes were from Metrohm. A personal computer was used for data storage and processing. The morphologies of the surface were observed in a Vega-Tescan electron microscope.

Preparation of Ru(III) complex–CNTs–GC and Ru(III)–GC-modified electrodes The GC electrode was first carefully polished with alumina (1.0 and 0.05 μm) on a polishing cloth. The electrode was placed in an ethanol container, and a bath ultrasonic cleaner was used to remove adsorbed particles. Then, 25 μl of DMSO–CNTs solutions (0.4 mg/ml) was cast on the surface of the GC electrode and dried in air to form a CNT film at the electrode surface. By immersing the GC electrode modified with CNTs in 0.1 mM ACN solution of Ru(III) complex for 5–30 s, a stable film of complex adsorbed on the surface of the electrode. After rinsing of the modified electrode with water, it can be used for electrochemical experiments immediately. The effective surface area of the electrodes modified with the immobilization of MWCNTs and SWCNTs were determined as 0.12 and 0.15 cm^2 from cyclic voltammograms of 1 mM $K_3[Fe(CN)_6]$ in phosphate buffer solution (pH7) [58]. To attach the Ru(III) complex to the surface of the GC electrode with the cyclic voltammetry technique, the GC electrode was carefully polished with alumina on a polishing cloth. With cycling of the potential between 0.1 and −0.5 V (30 cycles) at a scan rate of 100 mV s^{-1}, in an ACN solution containing 0.1 mM Ru(III) complex, a film of the Ru complex adsorbed on the electrode surface. For the adsorption of the complex on the surface of the reactivated GC electrode, the process was carried out in two steps. First, the GC electrode was held under a constant potential of 1.8 V for 5 min in 1 M H_2SO_4 solution. Second, the preanodized GC electrode was immersed in an ACN solution containing 0.1mM of Ru (III) complex for 1 h.

Results and discussions

Characterization of Ru complex-modified CNTs

Due to a large specific surface area of CNTs, a high quantity of Ru complexes can be adsorbed onto CNTs through strong π–π-stocking force between these two kind

of conjugated frames. Figure 1 shows the scanning electron microscope (SEM) images of MWCNTs and Ru complex-modified MWCNTs. It can be seen that the MWCNTs are very long and present as a highly entangled network structure, which is responsible for the difficulty to disperse CNTs in DMSO, due to low solubility of the CNTs in most solvents. Furthermore, the images reveal that the CNTs randomly distributed across the electrode surface. The inset of this figure shows the SEM image of the same sample with a higher magnification (the scale bar is about 200 nm). As we can see, the diameter of MWCNTs is about 15–20 nm. Figure 1b shows the SEM images of MWCNTs modified with the adsorption of Ru complex. The inset of this figure clearly shows that the diameters of more MWCNTs are about 40nm (two times of MWCNTs without Ru complex). They indicate that a high quantity of the Ru complex has adsorbed onto the surface of MWCNTs after immersing a MWCNT-modified electrode in the Ru complex solution.

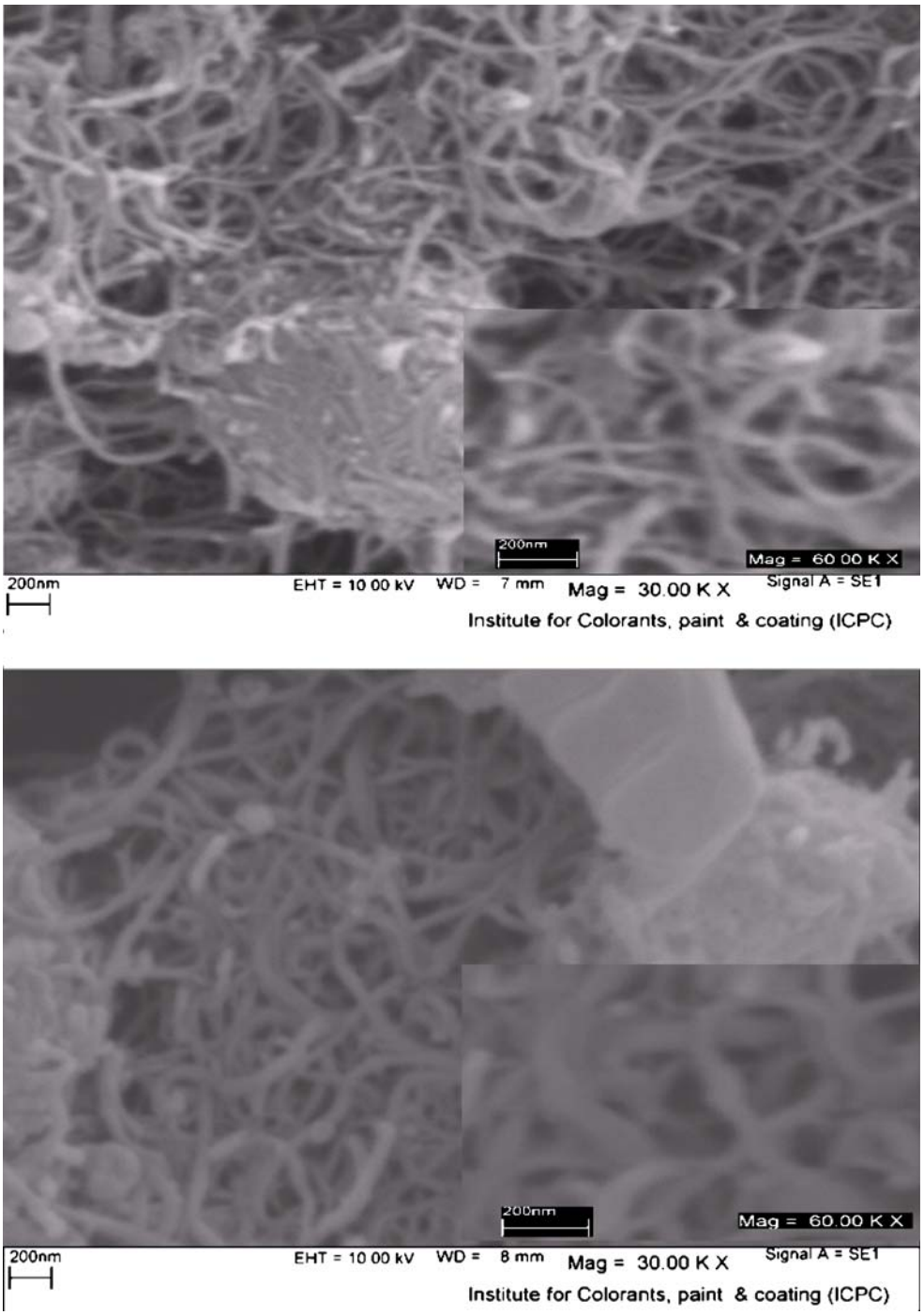

Fig. 1 *Up*, SEM image of the GC electrode modified with MWCNTs; *scale bar* is 200 nm. *Inset* is the SEM image with higher magnification for the same sample. *Down*, same as *up* for MWCNTS modified with Ru (III) complex–B

Electrochemical properties of Ru(III) complex–CNT-modified GC electrodes

Figure 2 shows the cyclic voltammograms of SWCNTs and SWCNTs/Ru(III) complex–B-modified GC electrodes at pH1 buffer solution (voltammograms a and b). For the SWCNTs/GC electrode, no redox peak between 1.0 and −0.6 V was found, and the background current was high. By immersing the electrode for 40 s in the complex solution, a thin layer of the Ru complex adsorbed on the surface of the CNT-modified GC electrode. Four independent GC electrodes were modified with CNTs and Ru complex with the same procedure. A well-defined redox couple with peak current 23.8 μA (±0.5) and peak potential separation less than 20 mV (± 2) was observed for the adsorbed complex. For the GC electrode modified with MWCNTs–Ru(III) complex, a cyclic voltammogram with a lower peak current, 10 μA (±0.4), and more peak potential separation, 100 mV (±5), was observed (Fig. 2 voltammogram d). No response was observed at the same potential range for the GC–MWCNT-modified electrode (Fig. 2 voltammogram c). SWCNTs can increase the surface area of the electrode; therefore, the background current and capacitances for the SWCNT-coated surface is higher than the GC electrode coated with MWCNTs. In addition, SWCNTs are highly permeable porous films, and electrolytes can penetrate through the film and gain access to the interior surface [59]. Figure 3a shows a cyclic voltammogram of the GC electrode modified with Ru complex–B, using consequence potential cycling (30 cycles at a scan rate of 100 mV s^{-1} between 0.1 and −0.5 V in 0.1 mM Ru(III) complex–B). As can be seen for the Ru complex-modified GC electrode, a voltammogram with small peak current, 1.1 μA, more peak potential separations, 100 mV, and higher background current was observed. For the GC electrode modified with immersing the preanodized electrode in the ACN solution containing 1 mM Ru complex–B during 60 min, a cyclic voltammogram with smaller peak current (0.1 μA) and high peak potential separation (70 mV) was observed (Fig. 3b). For voltammograms a and b, the peak separation between oxidation and reduction peaks is increased due to the increasing the resistance of the thicker film. However, observing a pair of well-defined redox couple with low peak potential separation (20 mV) indicates that the reversibility of the redox system is significantly improved. Due to high specific and conductive area of CNTs [60], the Ru complex more easily penetrates through the conductive porous channels of the electrode, leading to higher sensitivity. Figure 4 shows cyclic voltammograms of a SWCNTs–Ru(III) complex–B-modified GC electrode with different surface concentration of the complex, obtained by soaking the SWCNTs/GC electrode in 0.1 mM complex solution for different times. As shown in this figure, by immersing the electrode in the Ru complex solution for 10 s, a stable thin layer of complex adsorbed at the surface of electrode. By increasing the immersing time, the surface concentration of the Ru(III) complex is increased and then starts to level off after 40 s. In comparison to the GC electrode modified with SWCNTs, for the MWCNT-modified GC electrode at shorter period of immersing time, the peak currents level off (20 vs. 40 s). This is due to the fact that the effective surface area of SWCNTs is higher and they are highly permeable porous films and can adsorb more Ru complex molecules.

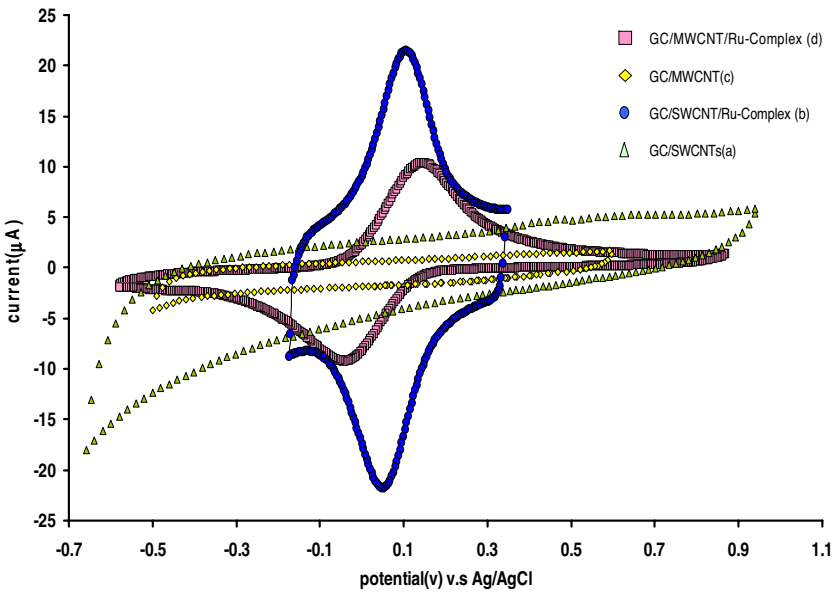

Fig. 2 *a* Cyclic voltammograms of a SWCNTs/GC-modified electrode in buffer solution (pH 1), *b* same as *a* for SWCNTs/Ru complex–B-modified electrode. *c*, *d* Same as *a* and *b* for MWCNTs, the immersing time for electrode modification is 40 and 20 s for GC electrodes covered with SWCNTs and MWCNTs, with a scan rate of 100 mV s^{-1}

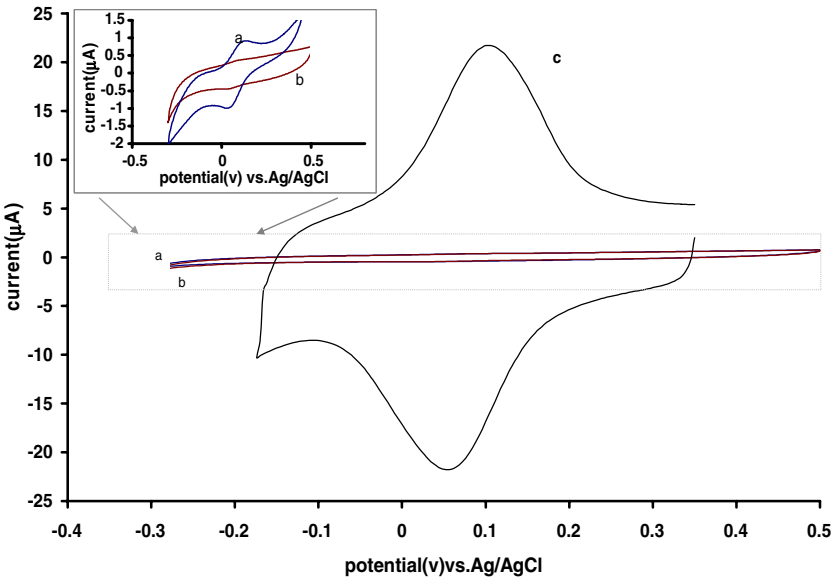

Fig. 3 Recorded cyclic voltammograms for GC electrode modified with Ru complex–B using consequence potential cycling (*a*), GC electrode modified with preanodization and physical adsorption of Ru complex (*b*), GC electrode modified with SWCNTs/Ru complex (*c*); scan rate, 100 mV s^{-1} in buffer solution (pH 1). *Inset* shows the enlarged of voltammogram *a* and *b*

Figure 5 shows cyclic voltammograms of the SWCNTs–Ru(III)–complex–B-modified GC electrode at different scan rates in buffer solution (pH1). As shown in insets of Fig. 5, at scan rates 10–1000 mV s^{-1}, the peak currents increased linearly with a sweep rate as expected for thin-layer electrochemistry process. Moreover, the anodic peak currents were almost the same as the corresponding cathodic peak currents, and the peak potential did not change with increasing the scan rate. The peak-to-peak potential separation is about 20 mV for sweep rates below 100 mV s^{-1}, suggesting facile charge transfer kinetics over this range of sweep rates. At higher sweep rates, the plot of peak currents versus the scan rate deviates from linearity, and the peak current becomes proportional to the square root of the scan rate (Fig. 5c), indicating a diffusion-controlled process, which is reflective of the relatively slow diffusion of counterions into the electrode surfaces. At higher sweep rates (v > 200 mV s^{-1}), peak separations begin to increase, indicating the limitation due to charge transfer kinetics. Based on the Laviron theory [61], the electron transfer rate constant (k_s) and charge transfer coefficient (α) can be determined by measuring the variation of the peak potential with the scan rate. The values of peak potentials were proportional to the logarithm

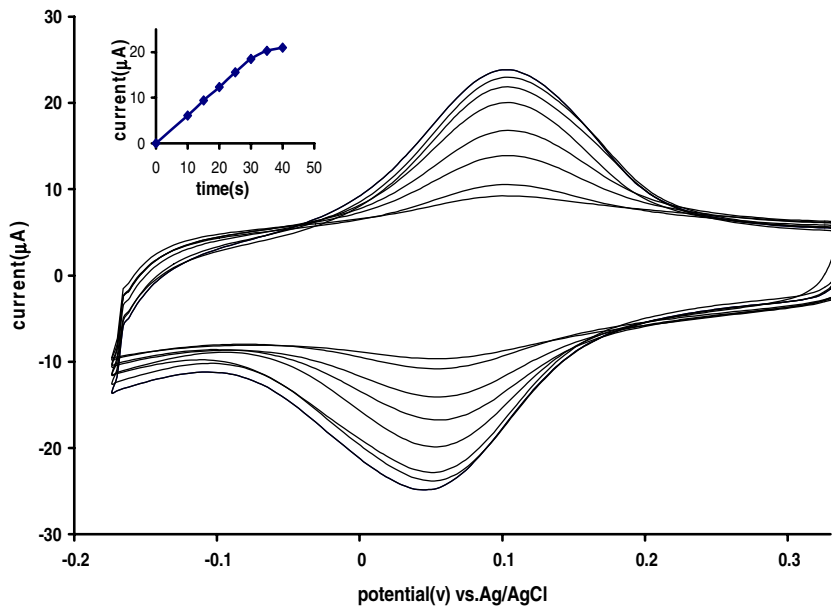

Fig. 4. Cyclic voltammetric responses of SWCNTs/Ru complex–B-modified GC electrode in buffer solution (pH 1) at scan rate 100 mV s^{-1} modified with immersion in 0.1 mM Ru complex for different times (from *inner* to *outer*) 10, 15, 20, 25, 30, 35, and 40 s. *Inset*, plot of peak currents vs. immersing time

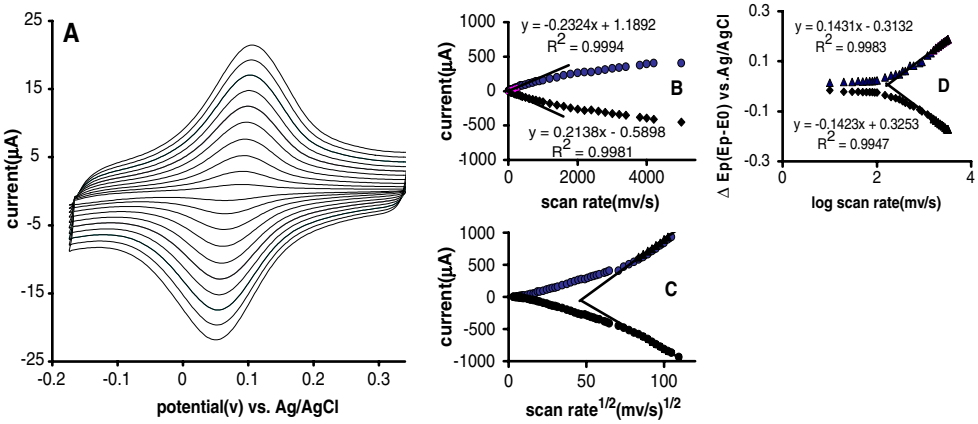

Fig. 5 **A** Cyclic voltammetric responses of SWCNTs/Ru complex–B-modified GC electrode in acidic buffer solution (pH 1) at scan rates (*inner* to *outer*) 10, 20, 30, 40, 50, 60, 70, 80, 90, and 100 mV s^{-1}. *Insets* (**B**, **C**), plots of peak currents vs. square root of scan rate and scan rate. **D** Variation of peak potential separation vs. log of scan rate

of the scan rate for scan rates higher than 2.0 V s^{-1} (Fig. 5D). The slope of the ΔE_{pc} vs. log (v) was about 142.3 mV. Using the equation $E_p = K - 2.3030(RT/\alpha nF)\log(v)$ and one electron transferred for Ru(III) complex, a charge transfer coefficient of α = 0.42 was obtained. Introducing this α value in the following equation [61], an apparent heterogeneous electron transfer rate constant, $k_s = 3.78s^{-1}$ (±0.20), was estimated.

$$\log k_s = \alpha\log(1-\alpha) + (1-\alpha)\log\alpha - \log(RT/nFv) - \alpha(1-\alpha)nFE/2.3RT \quad (1)$$

For other Ru(III) complexes used in this study (complexes A and C), the charge transfer and electron transfer rate constants on the surface GC electrodes modified with SWCNTs and MWCNTs are reported in Table 1. For the GC electrode modified with the adsorption of Ru complex–B, without using CNTs, the electron transfer rate constant is $2.2s^{-1}$. The large value of the electron transfer rate constant indicates the high ability of CNTs for promote an electron between the Ru complex and electrode surface. The surfaces of CNTs contain the large number of defects, and a special nanostructure of CNT may act as molecular wires to enhance the direct electron transfer of the Ru complex at CNT. The surface concentration of electroactive species, Γ, can be calculated from the slope of the plot of I_{pa} versus the scan rate (v < 100 mV s^{-1}) by the following equation [62]. The calculated value of Γ is 1.47 × 10^{-9}mol cm^{-2}.

$$I_p = n^2F^2vA\Gamma_c/4RT \quad (2)$$

where v is the sweep rate, A is the surface area, and the other symbols have their usual meaning. For other modified electrodes, the calculated Γ values are reported in Table 1. The working stability of the modified electrode was verified by monitoring the remaining amount of active substance after successive sweeps of cyclic voltammograms. The peak height and peak potential of the immobilized redox system during potential cycling over the range 0.55 to −0.2V remained nearly constant, and the amount of the ruthenium complex remaining on the electrode surface was almost 94% of its initial value after 200 cycles (Fig. 6). In addition, no significant decrease was observed after replacing the electrolyte used for 200 repetitive cycles with the fresh buffer solution. Furthermore, the storage stability of the chemically modified electrodes was very good. The electrodes were found to have reserved 97% of their initial activity for more than 1 month when kept in air at room temperature. The cyclic voltammogram of the GC electrode modified with the Ru complex, using consequence potential cycling technique, is recorded under the same condition. Although a well-defied redox couple was observed for the modified electrode, after 50 potential cycles, about 40% of the

Table 1 The values of α, k_s, and Γ for modified electrodes

CNT		SWNT			MWNT	
Complex	α	k_s (s^{-1})	$\Gamma\times10^{-9}$ (mol/cm^2)	α	k_s (s^{-1})	$\Gamma\times10^{-9}$ (mol/cm^2)
Complex (B)	0.44	3.83	1.193	0.41	3.73	0.642
Complex (A)	0.44	3.84	1.152	0.40	3.67	0.629
Complex (C)	0.45	3.85	1.147	0.4556	3.74	0.695

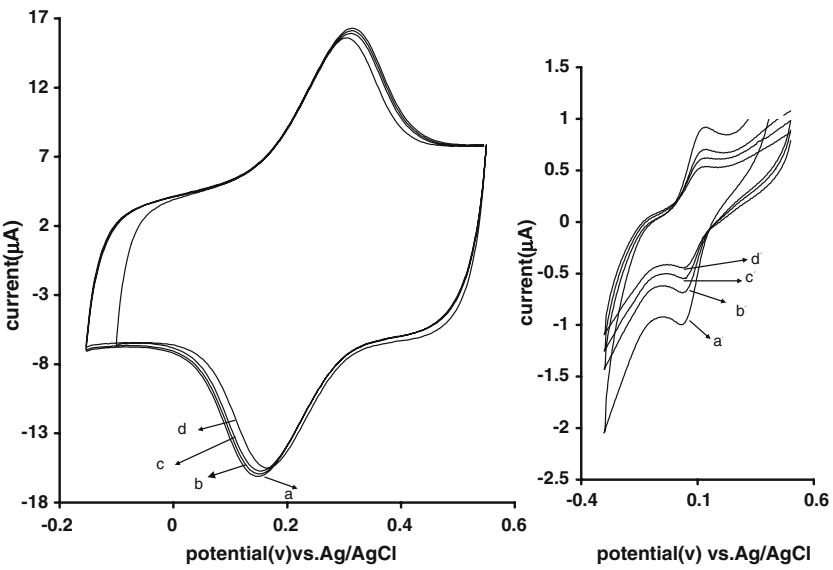

Fig. 6 *a* The first, *b* 20th, *c* 50th, and *d* 200th cyclic voltammograms of GC electrode modified with SWCNTs and Ru complex–B (immersing time for electrode modification 30 s) in acidic buffer solutions, pH 1. *Inset*, for the GC electrode modified with Ru complex–B, using consequence potential cycling for modification, *a′* first, *b′* 20th, *c′* 50th, and *d′* 100th; scan rate, 100 mV s^{-1}

adsorbed Ru complex remained at the electrode surface (inset of Fig. 6).

The high stability of the adsorbed Ru complex against desorption in aqueous solution is related to the chemical and mechanical stability of the nanotube film, the strong interaction of aromatic groups of the complex with π-staking of CNTs, and the possible interaction between the Ru complex and activated CNTs. To study the reproducibility of the electrode preparation procedure, five independent GC electrodes were modified with SWCNTs and the Ru complex. Cyclic voltammograms of prepared modified electrodes in the buffer solution were recorded. The relative standard deviation values of the measured cathodic peak currents were 4%. Due to the chemical stability, electrochemical reversibility, and high electron transfer rate constant of Ru complexes used in this study, they can be widely used in electrocatalysis as electron transfer mediators. We used one of the modified electrode, the GC electrode modified with $[Ru(NH_3)_5(2,4,5\text{-}Cl_3pcyd)](ClO_4)_2$ (complex B) and SWCNTs for the evaluation of the catalytic ability of the modified electrode in the electrocatalytic process.

The electrocatalytic reduction of NAD^+ at the GC electrode modified with Ru complex and SWCNTs

The catalytic reduction of NAD^+ at the Ru complex–SWCNT-modified GC electrode has been examined to evaluate the feasibility of using the electrodes in electrocatalysis as well

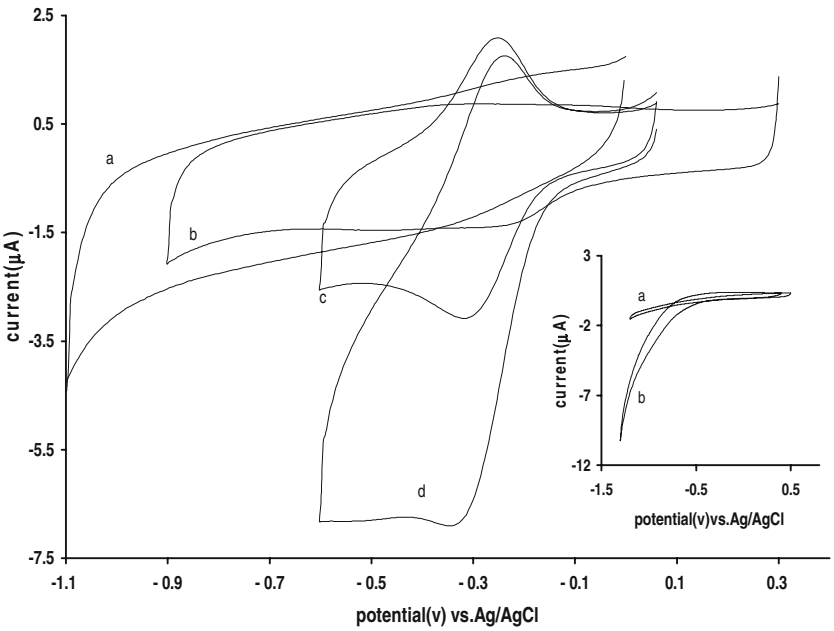

Fig. 7 *a* Cyclic voltammograms of the GC electrode modified with SWCNTs (*b*) as **a** in 0.5 μM NAD^+, *c*, *d* as *a* and *b* for SWCNTs/Ru complex–B-modified GC electrode, scan rate, 10 mV s^{-1} in phosphate buffer solution, pH 7. *Inset*, as voltammograms *a* and *b* for the bare GC electrode

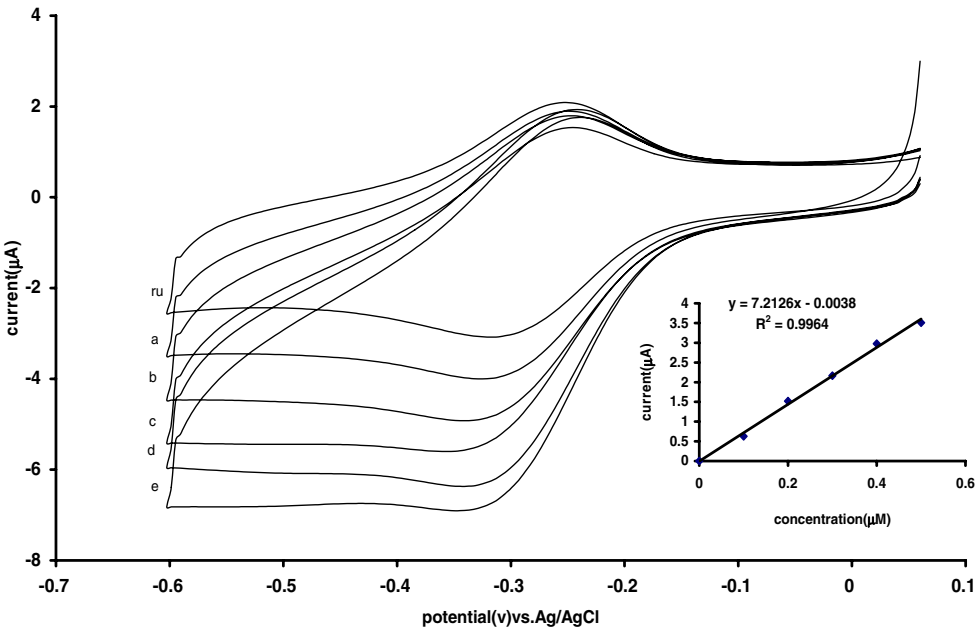

Fig. 8 *a*, *b* Recorded CV of Ru complex–B/SWCNT-modified GC electrode in the presence of different concentrations of NAD^+, scan rate, 10 mV s^{-1} in phosphate buffer solution, pH 7. *Inset*, Plot of peak currents vs. analyte concentration

as electroanalysis. One of the objectives of the current study was fabricating a modified electrode that is capable for the electrocatalytic reduction of NAD^+ to the enzymatically active compound NADH at a reduced overpotential. To test the electrocatalytic activity of the modified electrodes, the cyclic voltammograms were obtained in the absence and presence of NAD^+ in buffer solution (pH7). Figure 7 shows cyclic voltammograms of GC electrodes modified with SWCNTs and Ru complex–B + SWCNTs in buffer solution (pH7) free of and containing NAD^+. Upon the addition of 0.5 μM of NAD^+, there is a dramatic enhancement of the cathodic peak current, and the anodic peak currents decrease (Fig. 7d), which indicate a strong catalytic effect of the mediator for NAD^+ reduction. The cathodic peak current for NAD^+ reduction was observed at the SWCNT-modified GC electrode, but the peak current is about 15% of the response of the GC–SWCNTs–Ru complex-modified electrode under the same condition, and current decay is faster during consequence potential cycling. The inset of Fig. 7 shows the recorded cyclic voltammogram of the bare GC electrode in the absence and presence of NAD^+. As shown for the GC electrode, no cathodic response was observed for NAD^+ reduction until −0.7 V.

To optimize the electrocatalytic response of the modified electrode toward NAD^+ reduction, the effect of pH on the catalytic behavior of the modified electrode was investigated. The cyclic voltammograms of the modified electrode in 1 μM NAD^+ at different pH values (1 to 8) were recorded (not shown). At pH4 to 8, the modified electrode shows electrocatalytic activity, but higher peak currents are observed at pH7, and this value was chosen as optimized. Additionally, peak potentials are shifted to negative values with increasing pH values. Figure 8 shows cyclic voltammograms of the Ru complex/SWCNT-modified GC electrode in solutions containing different concentrations of NAD^+. The plot of the catalytic current vs. NAD^+ concentration was linear in the concentration range of 0.1–2 μM, which fitted the equation: $I_p = (\mu A) = 7.204 \mu A\, \mu M^{-1} - 0.0038\ \mu A$ and $R^2 = 0.9964$. The detection limit is 3nM when the signal-to-noise ratio is 3. Using a fixed concentration of 0.5 μM NAD^+ in the pH7 buffer solution, the peak current for the reduction of the analyte is proportional to the square root of the scan rate (not shown). These results indicate that at a sufficient potential, the reaction is controlled by the diffusion of the analyte. It can also be noted that by increasing the sweep rate, the peak potential for the catalytic reduction of NAD^+ shifts to more negative values, and a plot of peak current vs. the square root of the scan rate deviates from linearity, suggesting a kinetic limitation in the reaction between active sites of the Ru(II) complex and NAD^+. Based on the results, the following catalytic scheme (EC′ catalytic mechanism) describes the reduction of NAD^+

$$\mathrm{Ru(III)-complex} + \mathrm{e^-} \rightarrow \mathrm{Ru(II)-complex} \quad (3)$$

$$2\mathrm{Ru(II)-complex} + \mathrm{NAD^+} + \mathrm{H^+} \xrightarrow{k_{Cat}} \mathrm{NADH} + 2\mathrm{Ru(III)-complex} \quad (4)$$

Under the above conditions for an EC′ mechanism, the Andrieux and Saveant theoretical model [63] can be used to calculate the catalytic rate constant. Based on this theory, a relation between the peak current and the concentration of

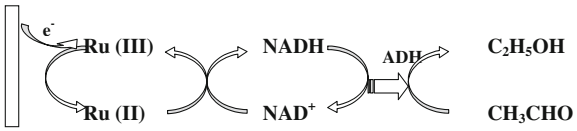

Scheme 2. Schematic representation of the ADH–CNTs–Ru complex biosensor for acetaldehyde detection

the substrate compound for the case of slow scan rates and a large catalytic rate constant exists:

$$I_p = 0.446nFAD^{\frac{1}{2}}\left(\frac{vF}{RT}\right)^{\frac{1}{2}}C_s \quad (5)$$

where D and C_s are the diffusion coefficient ($cm^2\ s^{-1}$) and the bulk concentration (mol cm^{-3}) of the substrate (NAD^+), respectively, and other symbols have their usual meanings. Low values of k_{Cat} results in values of the coefficient lower than 0.446. For a low scan rate (5–20 mV s^{-1}), the average value of this coefficient was found to be 0.36 for the Ru(III) complex/SWCNT-modified GC electrode with a coverage of 1.193×10^{-9}mol cm^{-2} and an effective surface area (A) of 0.15cm^2 in 0.5 μM NAD^+ at the phosphate buffer solution (pH7). According to the approach of Andrieux and Saveant and using Fig. 1 of [63], the average value of k_{Cat} calculated is 1.38 (±0.2) × $10^3 M^{-1}\ s^{-1}$. Due to high catalytic rate constants, the Ru complex adsorbed onto SWCNTs can be used as an electron transfer mediator for the electrocatalytic reduction of NAD^+ to NADH.

The biocatalytic activity of the modified electrode in the presence alcohol dehydrogenase

Many dehydrogenase enzymes catalyze specifically the reactions of important analytes to generate NADH as an electrochemically detectable product. Conjugation of the electrochemical regeneration of NADH cofactor and dehydrogenase-catalyzed reactions allows one to develop both the biosensors for a great number of analytes and the biofuel cells with different fuels. The present results indicate that the modified electrode can catalyze the reduction of NAD^+ at a reduced overpotential. Since the enzymatic activity of NAD^+ is stereo-specific [9], it is important to recognize whether the product of NAD^+ is enzymatically active. For this purpose, the ADH was added to buffer solution (1 mg ml^{-1}) containing different concentrations of acetaldehyde. The present results show that the CNTs–Ru complex-modified electrode can catalyze the reduction of NAD^+ that is generated from the reaction of NADH and acetaldehyde catalyzed by ADH, as schematized in Scheme 2. Cyclic voltammograms of the modified electrode in the solution containing enzyme and different concentration of acetaldehyde in the presence and absence a constant concentration of NAD^+ were recorded (Fig. 9). As shown without NAD^+ in the solution, the cathodic peak current in the presence different concentrations of acetaldehyde (voltammograms b to d) is similar to the cathodic peak current of the modified electrode without acetaldehyde (voltammogram a). With the addition of NAD^+ to the

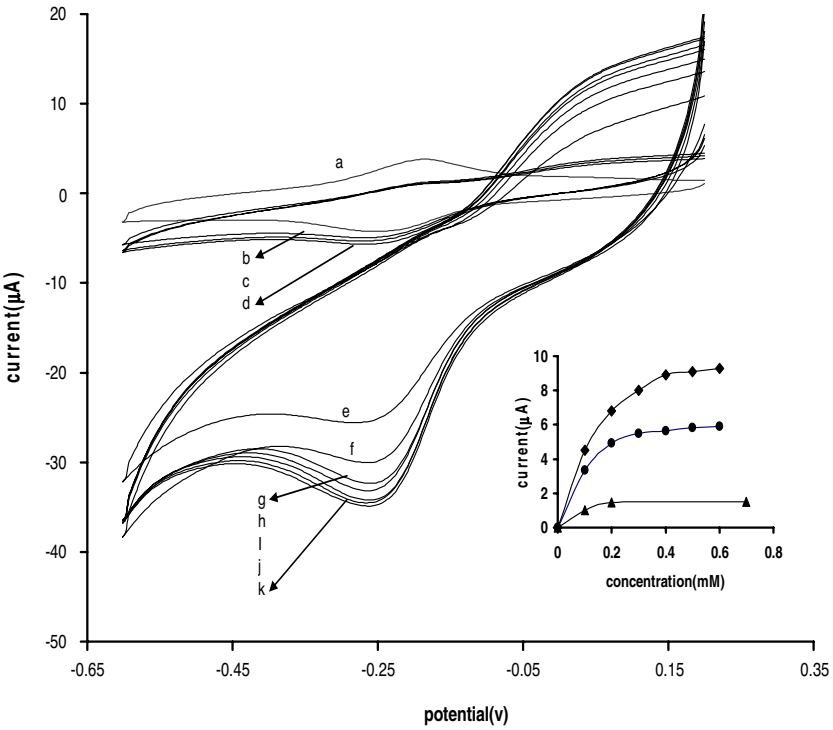

Fig. 9 Recorded CVs of Ru complex–B/SWCNT-modified GC electrode in buffer solution containing alcohol dehydrogenase enzyme (voltammogram *a*), voltammograms (*b*, *c*, and *d*) as voltammogram *a* in the presence 0.1, 0.2, and 0.7 mM of acetaldehyde, respectively. Voltammogram *e* as voltammogram *a* in the presence 0.1 mM of NAD^+. Voltammograms *f* to *k* as voltammograms *e* in the presence 0.1, 0.2, 0.3, 0.4, 0.5, and 0.6 mM of acetaldehyde, respectively. Electrolyte is phosphate buffer solution (pH 7), and scan rate is 20 mV s^{-1}. *Insets* is calibration curves of the biosensor in the presence different concentration of acetaldehyde, without NAD^+ (*triangles*) and in the presence 0.1 (*circles*) and 0.2 mM (*squares*) of NAD^+

solution, the cathodic peak currents increased with increasing acetaldehyde concentration (voltammograms f to k). These results indicate if the product of NAD^+ electroreduction is an enzymatically active derivate (NADH), it could be reoxidized by ADH. Under this condition, after substrate (acetaldehyde) addition, the enzymatic regeneration of the cofactor causes an increase in NAD^+ concentration at the electrode surface. As a result, the cathodic current of NAD^+ reduction will be increased. Since the NAD^+ and mediator concentrations are constant, the increase in the electrocatalytic current depends only on the acetaldehyde concentration. This characteristic was used as the base of the biosensor development for acetaldehyde determination. The inset of Fig. 9 shows the calibration curves of the modified electrode in the presence NAD^+ (0.1 and 0.2 mM), ADH, and different concentrations of acetaldehyde. As shown, the cathodic peak current of the biosensor is dependent on both acetaldehyde and NAD^+ concentration. The response of the biosensor for acetaldehyde detection in the absence of NAD^+ is not significant. Based on the above results, the main product of NAD^+ electroreduction at the modified electrode is the enzymatically active 1,4-NADH.

Conclusions

A simple, fast, reproducible, and direct procedure was used for adsorption of Ru(III) complexes as an electron transfer mediator on the GC electrode modified with CNTs. By immersing the GC electrode modified with the immobilization of CNTs in the Ru complex solution at less than 1 min, a stable thin film of the complex adsorbed strongly and irreversibly on the surface of the electrode. The GC electrode modified with the thin film of CNTs/Ru complex shows a stable and reproducible redox system with long stability, high electron transfer rate constant, and excellent electrochemical reversibility. Due to unique properties of CNTs and the Ru complex, especially synergistic effects between CNTs and the Ru(III) complex, the electrochemical properties of the produced nanocomposite significantly improved. The immobilized Ru(III)/Ru(II) redox couple can be used in electrocatalysis as electron transfer mediators. Compared with CNT- or Ru(III) complex-modified electrodes, the Ru complex–CNT–modified electrode shows high and excellent catalytic activity for the electroreduction of NAD^+ to the enzymatically active compound, 1,4-NADH. The combination of CNTs with Ru center is promising for a wide range of the biosensor in relation to the determination of the substrate is based on the electrochemical reduction of NAD^+ produced in an enzymatic reaction. The modified film in the presence of ADH enzyme can be used for detection of acetaldehyde with high sensitivity. Furthermore, this simple method can be used to prepare other organometallic complex-doped devices with high performance for the development of high-efficiency full cells and bioreactors.

Acknowledgments The financial supports of Iranian Nanotechnology inventive and Research Office of University of Kurdistan are gratefully acknowledged.

References

1. Aizawa M, Suzuki S, Kubo M (1976) Biochim Biophys Acta 444:886
2. Moiroux J, Deycard S, Malinski T (1985) J Electroanal Chem 194:99
3. Studnickova M, Klukanova HP, Turanek J, Kovar J (1988) J Electroanal Chem 252:383
4. Karyakin AA, Bobrova OA, Karyakina EE (1995) J Electroanal Chem 399:179
5. Damin A, Omanovic S (2006) J Mol Cat A Chem 253:222
6. Chen SM, Lin KH (2006) J Electroanal Chem 586:145
7. Chen SM, Lin KH (2005) J Electroanal Chem 583:248
8. Lin KC, Chen SM (2005) J Electroanal Chem 578:213
9. Karyakin AA, Bobrova OA, Karyakina EE (1995) J Electroanal Chem 399:179
10. Karyakin AA, Ivanova YN, Karyakina EE (2003) Electrochem Commun 5:677
11. Warriner K, Higson S Vadgama P (1997) Mater Sci Eng C 5:91
12. Beley M, Collin JP (1993) J Mol Catal 79:133
13. Man F, Omanovic S (2004) J Electroanal Chem 568:301
14. Damian A, Omanovic S (2006) J Mol Cat A: Chem 253:222
15. Lin KC, Chen SM (2006) J Electroanal Chem 589:52
16. Chen SM, Lin KH (2006) Electrochim Acta 51:4744
17. Sobolov SB, Leonida MD, Bartoszko-Malik A, Voivodov KI, McKinney F, Kim J, Fry AJ (1996) J Org Chem 61:2125
18. Voivodov KI, Sobolov SB, Leonida MD, Fry AJ (1995) Bioorg Med Chem Lett 5:681
19. Kim S, Yun SE, Kang C (1999) J Electroanal Chem 465:153
20. Kim S, Yun SE, Kang C (1999) Electrochem Commun 1:151
21. Cotton FA, Wilkinson G (1999) Advanced inorganic chemistry. Wiley, New York, pp 868–900
22. Appelbaum L, Heinriches C, Demtschuk J, Michman M, Oron M, Schafer HJ, Schumann H (1999) J Organomet Chem 592:240
23. Trasatti S (2000) Electrochim Acta 45:2377
24. Kim IH, Kim KB (2004) J Electrochem Soc 151:E7
25. Lima EC, Fenga PG, Romero JR, De- Giovani WF (1998) Polyhedron 17:313
26. Rodriguez M, Romero I, Liobet A, Deronzier AS, Parella T, Stoecki-Evans H (2001) Inorg Chem 40:4150
27. Premkumar J, Khoo SB (2004) Electrochem Commun 6:984
28. Wang X, Zhang Q, Han Z, Wang E, Guo Y, Hu C (2004) J Electroanal Chem 563:221
29. Azem A, Man F, Omanovic S (2004) J Molcul Cat A Chem 219:283
30. Salimi A, Pourbeyram S (2003) Talanta 60:205
31. Yan YK, Melchart M, Habtemariam A (2006) J Biol Inorg Chem 11:483
32. Polyanski D, Cabelli D, Muckerman JT, Fujita E, Koizumi TA, Fukushima T, Wada T, Tanaka K (2007) Angew Chem Int Ed 46:4169
33. Yakabson BI, Smally RE (1997) Am Sci 85:324
34. Lawrence NS, Wang J (2005) Electrochem Commun 8:71
35. Sun D, Zhu L, Huang H, Zhu G (2006) J Electroanal Chem 597:39

36. Zhao K, Song H, Zhung S, Dai L, He P, Fang Y (2007) Electrochem Commun 9:65
37. Li Z, Chen J, Pan D, Tao W, Nie L, Yao S (2006) Electrochim Acta 51:4255
38. Czerw R, Guo Z, Ajayan PM, Sun YP, Carol DL (2001) Nano Lett 1:423
39. Kooi SE, Schlecht U, Burghard M, Kern K (2002) Angew Chem 114:1409
40. Chen J, Liu H, Weimer WA, Halls MD, Waldeck DH, Walker GC (2002) J Am Chem Soc 124:9034
41. Chen RJ, Zhang Y, Wang D, Dai H (2001) J Am Chem Soc 123:3838
42. Frehill F, Vos JG, Benrezzak S, Koos AA, Konya Z, Ruther MG, Blau WJ, Fonseca A, Nagy JB, Biro LP, Minett AI, Panhuis M (2002) J Am Chem Soc 124:13694
43. Wang J (2005) Electroanalysis 17:7
44. Sherigara BS, Kutner W, Souza FD (2003) Electroanalysis 15:753
45. Davis JJ, Green MLH, Hill HAO, Leung YC, Sadler JO, Sloan JSC, Tsang SC (1998) Inorg Chim Acta 272:261
46. Tsang SC, Davis JJ, Green MLH, Hill HAO, Leung YC, Sadler JP (1995) J Chem Soc Chem Commun 1803
47. Davis JJ, Coles RJ, Hill HAO (1997) J Electroanal Chem 440:279
48. Wang J, Chen G, Wang M, Chatrathi MP (2004) Analyst 129:512
49. Hrapovic S, Liu YL, Male KB, Luong JHT (2004) Anal Chem 76:1083
50. Salimi A, Noorbakhsh A, Ghadermarzi M (2007) Sens Actuators B 123:530
51. Salimi A, Hallaj R (2005) Talanta 66:967
52. Salimi A, Noorbakhsh A, Ghadermarzi M (2005) Anal Biochem 344:16
53. Salimi A, Noorbakhsh A, Soltanian S (2006) Electroanalysis 18:16
54. Salimi A, Mamkhezri H, Mohebbi S (2006) Electrochem Commun 8:688
55. Sullivan BP, Calvert JM, Meyer TJ (1980) Inorg Chem 19:1404
56. Crutchley RJ, McCaw K, Lee FL, Gabe EJ (1990) Inorg Chem 29:2576
57. Bodige S, Mac Donnell FM (1997) Tetrahedron Lett 38:8159
58. Bard AJ, Faulkner LR (2001) Electrochemical methods, fundamentals and applications. Wiley, New York, p 231
59. Li J, Cassell A, Delzeit L, Han J, Meyyapan M (2002) J Phys Chem B 106:9299
60. Peigney A, Laurent C, Flahaut E, Bacsa RR, Rousset A (2001) Carbon 47:507
61. Laviron E (1974) J Electroanal Chem 52:355
62. Wang J (1994) Analytical electrochemistry. VCH, New York
63. Andriex CP, Saveant JM (1978) J Electroanal Chem 93:163